

# Effect of *Helichrysum italicum* on the Corrosion of Copper in Simulated Acid Rain Solution



This work is licensed under a Creative Commons Attribution 4.0 International License

Z. Pilić\* and I. Martinović

Department of Chemistry, Faculty of Science and Education, University of Mostar, Matice hrvatske bb, Mostar, Bosnia and Herzegovina

<https://doi.org/10.15255/CABEQ.2019.1614>

Original scientific paper  
Received: February 5, 2019  
Accepted: November 21, 2019

The inhibition of copper corrosion by *Helichrysum italicum* extract (HI) in simulated acid rain was investigated using electrochemical techniques. Results indicate an increase in corrosion inhibition efficiency with the HI extract concentration. The inhibitive process was assumed to occur via adsorption of the extract on the metal surface. The thermodynamic data indicated physical adsorption and followed the Freundlich isotherm. The effect of temperature on the copper corrosion was studied. The value of the activation energy confirmed physisorption of extract molecules on the copper surface. The concentration of Cu ions released into solution, measured by atomic absorption spectrometry, was in accordance with the electrochemical results.

**Keywords:**

copper, acid rain, corrosion, *Helichrysum italicum*

## Introduction

Copper and copper-based alloys are widely used in a great variety of applications, such as heat exchangers, building construction, electronics, art and cultural structures, etc.<sup>1–4</sup> However, when exposed to an urban polluted environment, such as acid rain<sup>5–9</sup>, these materials suffer from an acceleration of the corrosion process.

Extension of a structural material's life in a corroding environment is important. Corrosion and microbiologically influenced corrosion are a widespread problem. The economic significance is expressed in energy and efficiency loss, undesired accumulation of deposits, and adhesion of microorganisms to solids.

The corrosion behaviour of metals and alloys primarily depends on the properties of the surface oxide layer. The stability of the oxide film depends on a large number of variables, such as temperature<sup>10,11</sup>, chemical composition, and pH of the electrolyte<sup>12–14</sup>. A rainfall with pH < 5.6 is considered acid rain.

Acid-rain corrosion of outdoor-structures has become an actual problem and corrosion control is an essential issue regarding application. There are several ways of conferring protection, like formation of anodic films and treatment with organic in-

hibitors. One of the methods used very often to prevent corrosion is the use of corrosion inhibitors<sup>15–17</sup>.

The protection of copper and its alloys against corrosion with different kinds of inhibitors has been widely studied<sup>17–19</sup>; however, many commercial inhibitors are toxic and have an adverse effect on the environment, which limits their use. In the last decades, plant extracts containing compounds with nitrogen, sulphur and oxygen have been used as naturally occurring corrosion inhibitors that are environmentally friendly, easily biodegradable, inexpensive, and readily available.

Numerous studies have reported that natural corrosion inhibitors are mostly obtained from medicinal plants, aromatic spices and herbs, such as *Achillea millefolium* L.<sup>20</sup>, *Tannin*<sup>21,22</sup>, *Satureja montana* L.<sup>22</sup>, *Helichrysum italicum*<sup>23</sup> and others<sup>24</sup>. Protection efficiency of vegetal organic inhibitors is attributed mainly to the presence of a polar group acting as an active centre for adsorption. In addition, analysis of *Helichrysum italicum* confirmed presence of these compounds (acids, phenols) in plant material<sup>25</sup>.

The goal of the present work was to evaluate the inhibitive effect of *Helichrysum italicum* (Roth) G. Don as a green corrosion inhibitor on copper in acid rain. *Helichrysum italicum* (HI) is widely used in folk medicine and cosmetics. It is a medicinal plant of Mediterranean origin with outstanding antioxidant, antifungal, antibacterial<sup>26,27</sup> and anti-corrosion activity<sup>23</sup>.

\*Corresponding author: E-mail: zora.pilic@fpmoz.sum.ba

## Experimental details

Copper (Cu) 99.97 % (Ag, Bi, Pb, Sb, As, Fe, Ni, Sn, Zn, S, Se, Te as trace elements) was used for preparing working electrode. The surface area of the Cu exposed to the electrolyte was 0.502 cm<sup>2</sup>. The electrode was mechanically abraded by 1200 grade emery paper, degreased with ethanol in an ultrasonic bath, and rinsed with ultra-pure water (18.2 MΩ cm, produced by Millipore Simplicity UV Water Purification System). Prior to each measurement, the Cu electrode was polarized at –1.50 V vs. Ag | AgCl | 3 mol L<sup>-1</sup> KCl electrode for 15 seconds to remove air-formed surface oxide.

The electrochemical measurements were performed at 20 °C in a standard three-electrode cell. The counter electrode was a platinum electrode, and the reference electrode to which all potentials in the paper are referred, was an Ag | AgCl | 3 mol L<sup>-1</sup> KCl.

The electrolyte was a simulated acid rain solution. Chemical composition of the simulated acid rain<sup>28</sup> is given in Table 1. The pH value of solution was 4.5, and an electrical conductivity 1.306 mS cm<sup>-1</sup>. The pH value was adjusted by addition of the appropriate amount of 0.5 mol L<sup>-1</sup> H<sub>2</sub>SO<sub>4</sub>. All chemicals were of *p.a.* purity, and obtained from Sigma Aldrich.

Experiments were performed in a simulated acid rain solution, pH 4.5, with and without addition of *Helichrysum italicum*. The aerial parts of the *Helichrysum italicum* were collected during summer 2017, in Čapljina, B&H. The HI specimens were dried in air for two weeks. An extract of plant material was prepared after 3 h maceration in simulated acid rain at room temperature. The mass concentration of the *Helichrysum italicum* dry specimen in the macerate solution was 1.00 g L<sup>-1</sup> (1 g HI was added in 1 L acid rain solution). From this solution, lower concentrations were prepared by macerate dilution to 0.01, 0.10 and 0.50 g L<sup>-1</sup>.

The formation and stability of an oxide film on the copper in simulated acid rain solution were studied by the combination of electrochemical techniques, potentiodynamic polarization measurement (PP), cyclic voltammetry (CV), and electrochemical impedance spectroscopy (EIS). All measurements were performed with an Autolab PGSTAT320N controlled by a personal computer using Nova 1.5 software.

The PP measurements were performed in the potential range from –0.20 V to 0.20 V near corro-

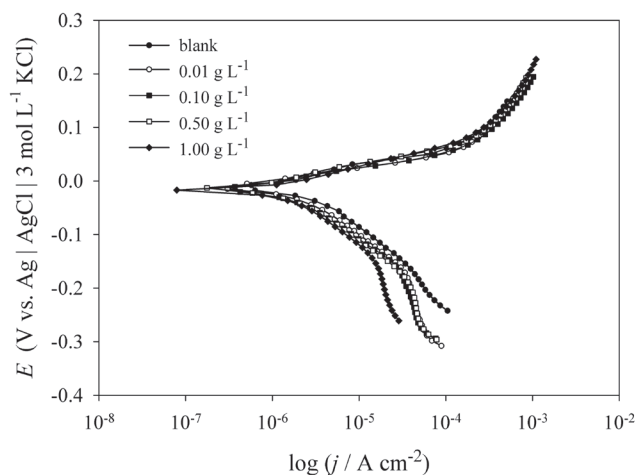


Fig. 1 – Potentiodynamic polarisation curves for the Cu electrode in simulated acid rain solution, pH 4.5, containing different concentrations of HI extract (shown in figure);  $\nu = 1 \text{ mV s}^{-1}$

sion potential with a scan rate of 1.0 mV s<sup>-1</sup>. The CV measurements were carried out in the potential range between –1.50 V and 0.20 V.

The EIS measurements were carried out in the frequency range between 10 kHz and 5 mHz with the *ac* amplitude  $\pm 10$  mV at constant potential. EIS measurements were performed at open circuit potential. Prior to each measurement, the electrode was stabilized for 30 min at open circuit potential. This procedure gave good reproducibility of results.

The concentrations of metallic ions released into acid rain solution after 60 minutes of specimen immersion at open circuit potential were obtained by atomic absorption spectrometry (AAS). Since the EIS measurements lasted approx. 60 minutes, the concentration of released ions was determined after this time.

## Results and discussion

### Potentiodynamic polarization

The potentiodynamic polarization curves obtained for the copper electrode in a simulated acid rain solution, pH 4.5, in the presence and absence of various concentrations of *Helichrysum italicum* extract are shown in Fig. 1. The comparison of the curves showed that the behaviour of copper was a function of HI concentration. The addition of extract induced changes in the cathodic current densities, but in the anodic domain, the current density remained almost the same compared with those in

Table 1 – Chemical composition of the simulated acid rain solution, g L<sup>-1</sup>

| NH <sub>4</sub> NO <sub>3</sub> | MgSO <sub>4</sub> · 7H <sub>2</sub> O | Na <sub>2</sub> SO <sub>4</sub> | KHCO <sub>3</sub> | CaCl <sub>2</sub> · 2H <sub>2</sub> O |
|---------------------------------|---------------------------------------|---------------------------------|-------------------|---------------------------------------|
| 0.13                            | 0.31                                  | 0.25                            | 0.13              | 0.31                                  |

Table 2 – Electrochemical parameters (polarization measurements) and calculated values of surface coverage,  $\theta$ , and inhibition efficiency,  $\eta$ , obtained from data shown in Fig. 1

| Solution<br>$\gamma/\text{g L}^{-1}$ | $E_{\text{corr}}/\text{V}$ | $j_{\text{corr}}/\text{A cm}^{-2}$ | $b_c$<br>$\text{V dec}^{-1}$ | $b_a$<br>$\text{V dec}^{-1}$ | $\theta$ | $\eta/\%$ |
|--------------------------------------|----------------------------|------------------------------------|------------------------------|------------------------------|----------|-----------|
| Blank                                | -0.001                     | $1.34 \cdot 10^{-6}$               | 0.051                        | 0.076                        | –        | –         |
| 0.01                                 | -0.004                     | $1.18 \cdot 10^{-6}$               | 0.056                        | 0.081                        | 0.119    | 11.9      |
| 0.10                                 | -0.006                     | $1.03 \cdot 10^{-6}$               | 0.063                        | 0.086                        | 0.231    | 23.1      |
| 0.50                                 | -0.011                     | $9.57 \cdot 10^{-7}$               | 0.059                        | 0.084                        | 0.286    | 28.6      |
| 1.00                                 | -0.018                     | $8.74 \cdot 10^{-7}$               | 0.083                        | 0.085                        | 0.348    | 34.8      |

pure solution. The modification caused by addition of the HI extract was a negative shift on the corrosion potential and a leftward displacement in the cathodic branch of the curves. This means that the HI extract acted as a cathodic type inhibitor of Cu under the given conditions.

The corresponding electrochemical polarization parameters of copper in an acid rain solution with and without presence of different HI concentrations, including corrosion potential,  $E_{\text{corr}}$ , corrosion current density,  $j_{\text{corr}}$ , cathodic Tafel slope,  $b_c$ , anodic Tafel slope,  $b_a$ , surface coverage,  $\theta$ , and inhibition efficiency,  $\eta$  are shown in Table 2. The surface coverage and inhibition efficiency were determined from corrosion current densities obtained by an intersection of cathodic and anodic Tafel lines, according to the equation:

$$\theta = \frac{j_{\text{corr},0} - j_{\text{corr,HI}}}{j_{\text{corr},0}} \quad (1)$$

$$\eta = \theta \cdot 100 \quad (2)$$

where  $j_{\text{corr},0}$  and  $j_{\text{corr,HI}}$  represent the corrosion current densities of the Cu electrode in the absence and presence of the HI extract, respectively.

It can be seen from Table 2 that the addition of HI extract showed some degree of inhibition, as evident by the  $\eta$  ranged from 11.9 % to 34.8 %, although only a low concentration of the extract was added. Highest  $\eta$ , 34.8 %, was given by addition of 1.00 g L<sup>-1</sup> extract to the acid rain medium.

Recently, we have investigated the corrosion inhibition of iron in a simulated acid rain solution using *Helichrysum italicum* extract. We have reported<sup>22</sup> that, in the presence of this extract, the inhibition efficiency was around 43 % at the concentration of 1.00 g L<sup>-1</sup>.

The corrosion potential values (Table 2) show that the addition of HI extract shifts the corrosion potential towards the cathodic direction and no significant change is observed for the corrosion potential in the presence of the extract. Further inspection of the table reveals that both Tafel slopes increase

with increasing extract concentration. This result suggests that the presence of the extract affects the anodic as well as the cathodic process, while the cathodic current densities decrease is more pronounced. It is also worth noting that the value of  $b_c$  changes with the addition of extract more than does the value of  $b_a$ , which indicates that the HI extract behaves cathodically rather than anodically.

The inhibitor may affect either one or both of the anodic and cathodic processes. When the change in the  $E_{\text{corr}}$  value is greater than 85 mV, an inhibitor can be classified as anodic or cathodic. Inhibitors that cause a shift of less than 85 mV in the  $E_{\text{corr}}$  are mentioned as mixed-type inhibitors<sup>29</sup>. In our study, the largest displacement in  $E_{\text{corr}}$  value was approximately 17 mV. The values of Tafel slope remained more or less constant in the presence of inhibitor, suggesting that the effect of inhibitor was not as large as to change the mechanism of corrosion. According to the literature<sup>30</sup>, this inhibition effect is merely the blocking of surface active sites due to adsorption of molecules from extract.

### Cyclic voltammetry

The cyclic voltammograms obtained for Cu electrode in the simulated acid rain with and without the HI extract are presented in Fig. 2. It can be seen that the oxide growth starts at potentials positive to -0.40 V. Cyclic voltammograms show two anodic current peaks,  $A_1$  and  $A_2$ . The first anodic peak,  $A_1$  at -0.20 V, can be attributed to the electroformation of a hydrous  $\text{Cu}_2\text{O}$  layer<sup>31,32</sup>. The second anodic peak,  $A_2$  at around 0.10 V, can be ascribed to the formation of CuO oxide<sup>31</sup>. In the cathodic direction, three peaks were observed. The cathodic peak  $C_3$  at -0.20 V can be assigned to the electroreduction of CuO to  $\text{Cu}_2\text{O}$ , while peak  $C_2$  at -0.70 V can be attributed to the reduction of  $\text{Cu}_2\text{O}$  to Cu. The third cathodic peak,  $C_1$  has been associated to the reduction of soluble Cu(I) species<sup>33</sup>.

It can be seen from the cyclic voltammogram recorded in the presence of the HI extract that the oxidation process from Cu(I) to Cu(II) is inhibited, resulting in the total anodic charge,  $Q_A$  being decreased. Anodic charges determined with and without the addition of *Helichrysum italicum* extract were used to calculate the surface coverage,  $\theta$  according to equation:

$$\theta = \frac{Q_{A,0} - Q_{A,HI}}{Q_{A,0}} \quad (3)$$

where  $Q_{A,0}$  and  $Q_{A,HI}$  represent anodic charges in the absence and presence of the extract. Inhibition efficiency,  $\eta$ , was calculated according to equation (2), and presented in Table 3 together with the surface coverage values.

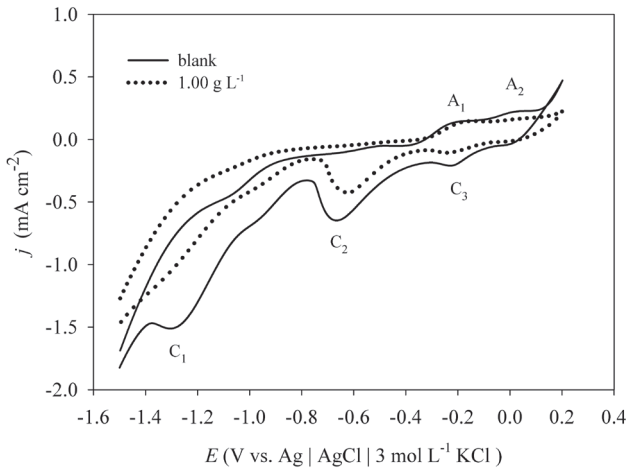


Fig. 2 – Cyclic voltammograms for the Cu electrode in simulated acid rain solution, pH 4.5, in presence and absence of the HI extract (shown in figure);  $v = 40 \text{ mV s}^{-1}$

Under the assumption that the surface layer is mostly composed of CuO oxide, its thickness,  $d$ , is calculated from the anodic charge,  $Q_A$ , corresponding to the surface layer oxidation, according to expression:

$$d = \frac{V_m \cdot Q_A}{z \cdot F \cdot \sigma} \quad (4)$$

where  $V_m$  is the molar volume of CuO<sup>34</sup> ( $V_m = 12.4 \text{ cm}^3 \text{ mol}^{-1}$ ),  $z$  is the number of electrons,  $F$  is the Faraday constant, and  $\sigma = 2$  is the roughness factor of the surface.

The values of surface coverage and inhibition efficiency follow the same trend as the values determined from the polarization measurements.

#### Adsorption isotherm and free energy of adsorption

The modes of the inhibition effect of the inhibitor depend not only on the inhibitor, but also on the nature and charge of the metal and type of electrolyte. For adsorption of organic compounds at the metal/solution interface, generally two modes are considered; physical adsorption and chemisorption. It is widely acknowledged that the adsorption isotherms provide an insight into the mechanism of corrosion inhibition. The degree of surface coverage values ( $\theta$ ) obtained from PP measurements (PP curves are presented only for 20 °C, Fig. 1) using the equations (1), assuming a direct relationship between surface coverage and inhibition efficiency, was tested graphically.

The obtained linear plots indicate that the experimental data fits the Freundlich adsorption isotherm (Fig. 3).

The relationship between the surface coverage,  $\theta$ , the equilibrium adsorption constant,  $K$ , and the

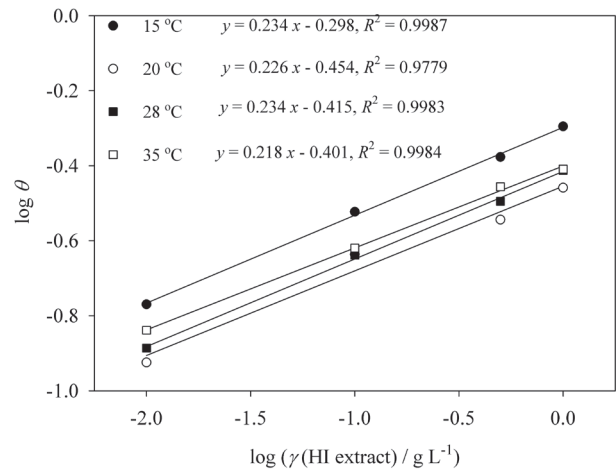


Fig. 3 – Freundlich adsorption isotherm for HI extract at different temperatures (shown in figure)

inhibitor concentration,  $\gamma$ , is given by the following equations:

$$\theta = K\gamma^n \quad (5)$$

where  $0 < n < 1$ , or

$$\log \theta = \log K + n \log \gamma \quad (6)$$

The equilibrium adsorption constant is related to the free energy of adsorption  $\Delta G^{\circ 20}$ :

$$\Delta G^{\circ} = -RT \ln[(1000(\text{g L}^{-1}) \cdot K(\text{L g}^{-1}))] \quad (7)$$

where the value of 1000 is the mass concentration of water in the solution in  $\text{g L}^{-1}$ ,  $R$  is the universal gas constant, and  $T$  is the absolute temperature. This multiplication was used to nullify the unit of  $K$  ( $\text{L g}^{-1}$ ) with 1000 g of water per L of aqueous solution.

The calculated values of free energy of adsorption from the PP data (Table 4) indicated a physical

Table 3 – Anodic charge, thickness of oxide film, surface coverage, and inhibition efficiency calculated from data shown in Fig. 2

| Solution<br>$\gamma/\text{g L}^{-1}$ | $Q_A/\text{mC cm}^{-2}$ | $d/\text{nm}$ | $\theta$ | $\eta/\%$ |
|--------------------------------------|-------------------------|---------------|----------|-----------|
| Blank                                | 13.335                  | 4.28          | –        |           |
| 1.00                                 | 8.785                   | 2.82          | 0.341    | 34.1      |

Table 4 – Values of Gibbs energy of HI extract adsorption on copper at different temperatures

| $T/^\circ\text{C}$ | $\Delta G^{\circ}/\text{kJ mol}^{-1}$ |
|--------------------|---------------------------------------|
| 15                 | –14.90                                |
| 20                 | –14.28                                |
| 28                 | –14.89                                |
| 35                 | –15.32                                |

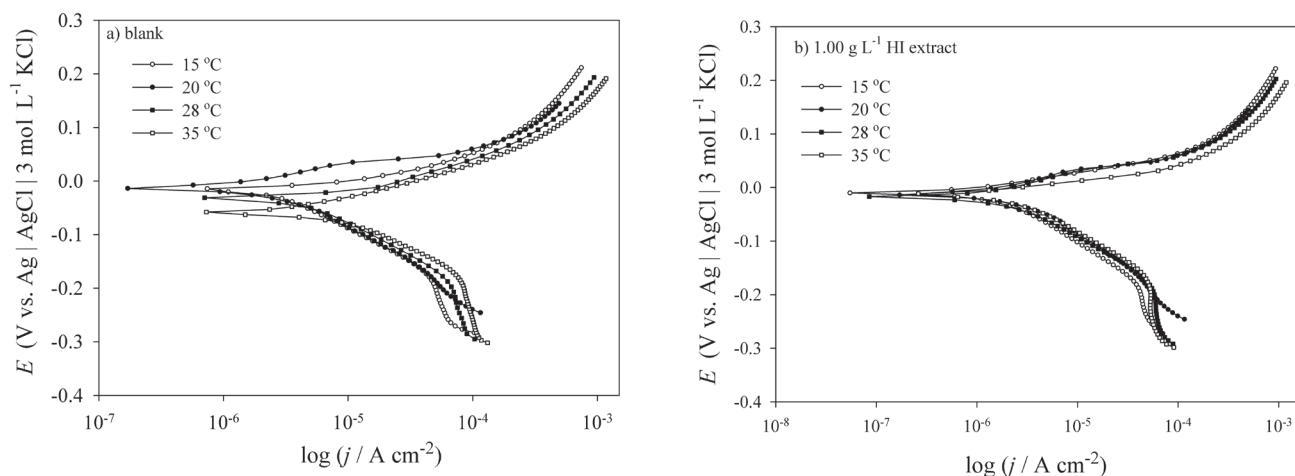


Fig. 4 – Effect of temperature on polarization curves of Cu corrosion rate in simulated acid rain solution a) without, and b) with  $1.00 \text{ g L}^{-1}$  HI extract

adsorption of organic compounds from the HI extract on the copper surface. The negative values of  $\Delta G^\circ$  ensured spontaneity of the adsorption process and stability of the adsorbed surface layer. Generally, values of the free energy of adsorption up to  $-20 \text{ kJ mol}^{-1}$  are consistent with electrostatic interactions between organic molecules and charged metal surface, and point to physical adsorption<sup>11,20,24</sup>.

### Effect of temperature

The effect of temperature on corrosion rate of copper was investigated in the temperature range  $15 - 35 \text{ }^\circ\text{C}$ . Fig. 4 shows the results of potentiodynamic polarization measurements for Cu in the simulated acid rain with and without  $1.00 \text{ g L}^{-1}$  HI extract at different temperatures. Table 5 shows the corresponding electrochemical polarization parameters of copper in acid rain solution with and without presence of  $1.00 \text{ g L}^{-1}$  HI at different temperatures.

Table 5 suggests that the inhibition efficiency drops from 50.7 % to 34.8 % when the temperature increases from 15 to 20  $^\circ\text{C}$ . Beyond 20  $^\circ\text{C}$ , the inhibition starts to increase again to 39.0 % at 35  $^\circ\text{C}$ .

The physisorption of inhibitor is favoured at lower temperatures, while chemisorption is favoured as temperature increases<sup>35</sup>. This increase in the inhibition efficiency along with the increase in temperature could be assigned to the change in the nature of the adsorption mode from physisorption to chemisorption<sup>35–37</sup>. The increased inhibition efficiency with the temperature increase could also be explained as the likely specific interaction between inhibitor molecule and the metal substrate<sup>35,38,39</sup>.

In order to calculate activation energy, the Arrhenius equation was used:

$$j_{\text{corr}} = A \exp\left(\frac{-E_a}{RT}\right) \quad (8)$$

Table 5 – Electrochemical parameters (polarization measurements) and calculated values of surface coverage,  $\theta$ , and inhibition efficiency,  $\eta$ , obtained from data shown in Fig. 4

| Solution $\gamma/\text{g L}^{-1}$ | $T/^\circ\text{C}$ | $j_{\text{corr}}/\text{A cm}^{-2}$ | $\theta$ | $\eta/\%$ |
|-----------------------------------|--------------------|------------------------------------|----------|-----------|
| blank                             | 15                 | $1.27 \cdot 10^{-6}$               | –        | –         |
| blank                             | 20                 | $1.34 \cdot 10^{-6}$               | –        | –         |
| blank                             | 28                 | $3.36 \cdot 10^{-6}$               | –        | –         |
| blank                             | 35                 | $3.74 \cdot 10^{-6}$               | –        | –         |
| 1.00                              | 15                 | $6.26 \cdot 10^{-7}$               | 0.507    | 50.7      |
| 1.00                              | 20                 | $8.74 \cdot 10^{-7}$               | 0.348    | 34.8      |
| 1.00                              | 28                 | $2.06 \cdot 10^{-6}$               | 0.387    | 38.7      |
| 1.00                              | 35                 | $2.28 \cdot 10^{-6}$               | 0.390    | 39.0      |

Table 6 – Activation energy for Cu in simulated acid rain in the presence and absence of HI extract

| Solution $\gamma/\text{g L}^{-1}$ | $E_a/\text{kJ mol}^{-1}$ |
|-----------------------------------|--------------------------|
| blank                             | 40.3                     |
| 1.00                              | 46.8                     |

where  $A$  is the Arrhenius pre-exponential factor,  $T$  the absolute temperature,  $E_a$  the activation energy for the corrosion process, and  $R$  the universal gas constant.

The activation energy ( $E_a$ ) for Cu was determined by linear regression between  $\ln(j_{\text{corr}})$  and  $1/T$ , shown in Fig. 5, and the calculated values are shown in Table 6.

The higher value of the activation energy of the process in the presence of inhibitor when compared to that in their absence is attributed to its physisorption, while the opposite is the case with chemisorption<sup>40,41</sup>. The higher value of  $E_a$  in the presence of

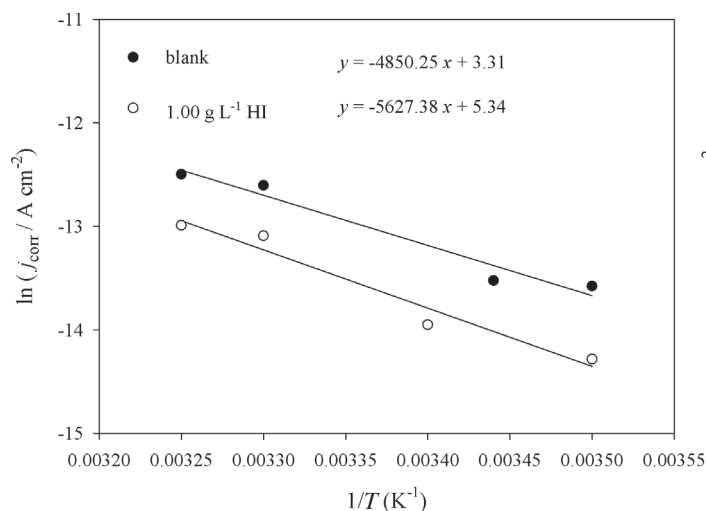


Fig. 5 – Arrhenius plots of Cu in simulated acid rain with and without 1.00 g L<sup>-1</sup> of HI extract

HI extract indicates that the inhibitors were adsorbed on the metal surface creating a physical barrier to charge and mass transfer.

#### Electrochemical impedance spectroscopy

Impedance measurements on the copper electrode in simulated acid rain, pH 4.5, in the presence (0.01, 0.10, 0.50 and 1.00 g L<sup>-1</sup>) and absence of *Helichrysum italicum* extract were performed at the open circuit potential. Impedance spectra are presented as Nyquist plots (Fig. 6). The impedance experimental data of the Cu electrode in pure acid rain solution and in the presence of the HI extracts were analysed by a fitting to the electric equivalent circuit (EEC), shown in detail in Fig. 6, and resulting values of EEC elements are given in Table 7. It consisted of an electrolyte resistance ( $R_{\Omega} \sim 50 \Omega \text{ cm}^2$ ) connected with two time constants. The first time constant, in the medium frequency range, is ascribed to charge transfer process of copper dissolution in simulated acid rain solution. The first time constant consisted of charge transfer resistance,  $R_1$ , and constant phase element,  $CPE_1$ , that replace ca-

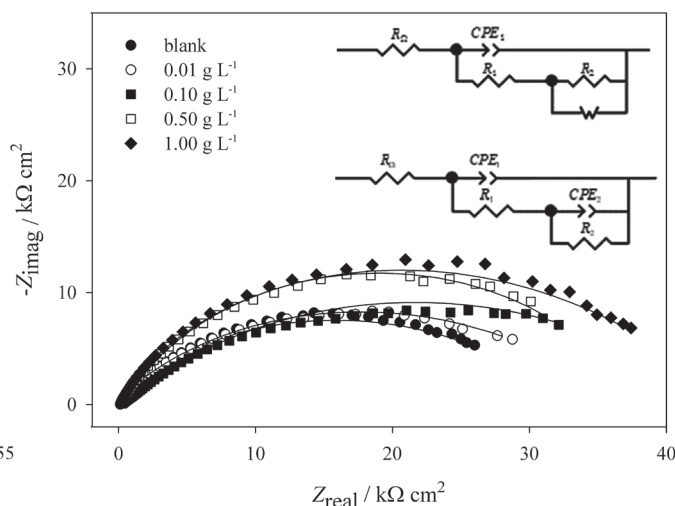


Fig. 6 – Impedance spectra (Nyquist plot) of the Cu electrode recorded at  $E_{OCP}$  in simulated acid rain solution, pH 4.5, containing different concentrations of HI extract (shown in figure)

capacity of electrochemical double layer. Its impedance may be defined:  $Z_{CPE}(\omega) = [Q(j\omega)^n]^{-1}$  where  $Q$  is a constant,  $\omega$  is the angular frequency, and  $n$  is the CPE power with values between 0.5 and 1. When  $n = 1$ , the CPE describes an ideal capacitor with  $Q$  equal to the capacitance. For  $0.5 < n < 1$ , the CPE describes a distribution of dielectric relaxation times in frequency space, and when  $n = 0.5$ , the CPE represents a Warburg impedance.

The second time constant, in the low frequency range, consisted of surface layer resistance,  $R_2$ , and Warburg element that indicate diffusion process through the film.

As may be seen from Table 7, the addition of increased concentrations of the HI extract led to the increase in charge transfer resistance,  $R_1$  (from 2.32 to 3.76 kΩ cm<sup>2</sup>) and surface layer resistance,  $R_2$  (from 30.52 to 45.15 kΩ cm<sup>2</sup>), and decrease in double layer capacity (from  $19.16 \cdot 10^{-6}$  to  $16.53 \cdot 10^{-6} \Omega^{-1} \text{ s}^n \text{ cm}^2$ ) and Warburg impedance (from  $69.85 \cdot 10^{-6}$  to  $48.84 \cdot 10^{-6} \Omega^{-1} \text{ s}^{0.5} \text{ cm}^2$ ). Decreased Warburg value means that the diffusion of species is reduced by adsorbed surface layer of HI extract. Observed behaviour is attributed to a decrease in a

Table 7 – Impedance parameters for Cu electrode in a simulated acid rain solution, pH 4.5, in the presence and absence of HI extracts

| $\gamma/\text{g L}^{-1}$ | $Q_1 \cdot 10^6 / \Omega^{-1} \text{ s}^n \text{ cm}^2$ | $n_1$ | $R_1 / \text{k}\Omega \text{ cm}^2$ | $R_2 / \text{k}\Omega \text{ cm}^2$ | $W \cdot 10^{-6} / \Omega^{-1} \text{ s}^{0.5} \text{ cm}^2$ | $Q_2 \cdot 10^6 / \Omega^{-1} \text{ s}^n \text{ cm}^2$ | $n_2$ | $\eta/\%$ |
|--------------------------|---|-------|-------------------------------------|-------------------------------------|--|---|-------|-----------|
| blank                    | 19.16   | 0.86  | 2.32                                | 30.52                               | 69.85  | –   | –     | –         |
| 0.01                     | 18.21   | 0.85  | 2.61                                | 31.54                               | –  | 75.64   | 0.43  | 11.1      |
| 0.10                     | 22.36   | 0.86  | 3.17                                | 34.26                               | –  | 68.88   | 0.41  | 26.8      |
| 0.50                     | 17.20   | 0.89  | 3.46                                | 35.54                               | –  | 54.75   | 0.44  | 32.9      |
| 1.00                     | 16.53   | 0.88  | 3.76                                | 45.15                               | –  | 48.84   | 0.60  | 38.3      |

local dielectric constant and/or an increase in the thickness of the double layer due to the adsorption of the HI extract constituents<sup>42,43</sup>.

The total impedance of the Cu electrode/acid rain interface in the presence and absence of the HI extract, recorded at the open circuit potential, is given by:

$$Z_{tot} = R_{\Omega} + \left[ Q_1 (j\omega)^{n_1} + \left( R_1 + \frac{R_2 W}{R_2 + W} \right)^{-1} \right]^{-1} \quad (9)$$

$$Z_{tot} = R_{\Omega} + \left( Q_1 (j\omega)^{n_1} + \left( R_1 + \frac{R_2}{R_2 Q_2 (j\omega)^{n_2} + 1} \right)^{-1} \right)^{-1} \quad (10)$$

The inhibition efficiency,  $\eta$ , can be calculated from charge transfer resistance values according to the following equation<sup>29</sup>:

$$\eta = \frac{R_{ct} - R_{ct}^0}{R_{ct}} \cdot 100 \quad (11)$$

where  $R_{ct}^0$  and  $R_{ct}$  are the charge transfer resistance of the Cu in the presence and absence of HI extract. The values of inhibition efficiency are presented in Table 7 and follow the same trend as the values determined from polarisation measurements and cyclic voltammetry.

### Copper concentration in acid rain solution

The quantities of Cu ions dissolved during 1 hour-immersion of the Cu specimen in acid rain solution at  $E_{OCP}$  with and without the HI extract were determined using the AAS technique. Generally, metal dissolution is dependent on metal/alloy itself and pH of solutions. The results obtained in static immersion tests are listed in Table 8.

As seen from Table 8, the quantity of the Cu released from the copper immersed in the pure acid

rain solution amounted to  $356.57 \mu\text{g L}^{-1} \text{cm}^{-2}$ . The addition of *Helichrysum italicum* extract reduced the quantity of Cu ions released in the solution. These results are in a good agreement with the results obtained by electrochemical techniques, and confirm the adsorption of organic compounds from the HI extract on the copper surface. The adsorption layer acted as an effective barrier between the Cu surface and the aggressive electrolyte.

### Conclusion

The inhibition effectiveness of *Helichrysum italicum* extract against copper corrosion in simulated acid rain was studied using electrochemical techniques. The aqueous extract of *Helichrysum italicum* showed very low inhibitive properties for Cu corrosion in the investigated electrolyte. The protection efficiency of HI extract increased along with the increase in HI concentration, showing maximal efficiency around 35 % at  $1 \text{ g L}^{-1}$ . The adsorption behaviour of the extract followed the Freundlich adsorption model. Physical adsorption between the HI extract and the copper surface was confirmed by the Gibbs energy value ( $\sim 15 \text{ kJ mol}^{-1}$ ). The adsorbed HI molecules acted as a physical barrier preventing the electrolyte from contacting the copper surface.

The value of energy activation,  $E_a$ , for simulated acid rain solution with the presence of  $1.00 \text{ g L}^{-1}$  of HI extract was calculated, and found to be  $46.8 \text{ kJ mol}^{-1}$ , while  $E_a$  for uninhibited simulated acid rain solution was found to be  $40.3 \text{ kJ mol}^{-1}$ . This increase in  $E_a$  value with the addition of HI extract is attributed to its physisorption on copper surface. According to the polarization measurements, the inhibition efficiency was the highest at the lowest temperature examined,  $15 \text{ }^\circ\text{C}$  ( $\eta = 50.7 \%$ ), and decreased with increasing electrolyte temperature.

According to the impedance results, resistance values increased (from  $32.84$  to  $48.91 \text{ k}\Omega \text{ cm}^2$ ), and double layer capacitance values decreased (from  $19.16 \cdot 10^{-6}$  to  $16.53 \cdot 10^{-6} \Omega^{-1} \text{ s}^n \text{ cm}^{-2}$ ), which can be ascribed to an increase in electrical double layer thickness. Atomic absorption spectrometry results showed that the addition of HI extract reduced the quantity of Cu ions released in the solution (from  $356.57$  to  $135.46 \mu\text{g L}^{-1} \text{cm}^{-2}$ ).

### ACKNOWLEDGMENT

The authors are grateful for the financial support of the Federal Ministry of Education and Science of Bosnia and Herzegovina.

Table 8 – Quantities of Cu ions dissolved during 1-hour immersion of the Cu specimen in acid rain solution at  $E_{OCP}$  containing *Helichrysum italicum* extract obtained from the AAS technique

| Solution $\gamma/\text{g L}^{-1}$ | Quantity of released Cu/ $\mu\text{g L}^{-1} \text{cm}^{-2}$ |
|-----------------------------------|--|
| Blank                             | 356.57   |
| 0.01                              | 254.94   |
| 0.10                              | 153.39   |
| 0.50                              | 141.43   |
| 1.00                              | 135.46   |

**List of symbols**

|                  |  |
|------------------|--|
| $A$              | – Arrhenius pre-exponential factor   |
| $b$              | – Tafel slope, $V \text{ dec}^{-1}$  |
| CPE              | – constant phase element   |
| $d$              | – film thickness, nm   |
| $E_a$            | – activation energy, $\text{kJ mol}^{-1}$  |
| $E$              | – potential, V   |
| $F$              | – Faraday constant, $\text{C mol}^{-1}$  |
| $f$              | – frequency, Hz  |
| $\Delta G^\circ$ | – free energy of adsorption, $\text{kJ mol}^{-1}$  |
| $j$              | – current density, $\text{A cm}^{-2}$  |
| $K$              | – equilibrium adsorption constant  |
| $n$              | – characteristic parameter of CPE  |
| $Q$              | – coefficient reflecting combination of properties related to surface and electroactive species, $\Omega^{-1} \text{ cm}^{-2} \text{ s}^n$ |
| $Q$              | – charge density, $\text{C cm}^{-2}$   |
| $R$              | – resistance, $\Omega \text{ cm}^2$  |
| $R$              | – universal gas constant, $8.314 \text{ J K}^{-1} \text{ mol}^{-1}$  |
| $T$              | – absolute temperature, K  |
| $V$              | – volume, $\text{cm}^3$  |
| $W$              | – Warburg impedance, $\Omega^{-1} \text{ s}^{0.5} \text{ cm}^{-2}$   |
| $Z$              | – impedance, $\Omega \text{ cm}^2$   |
| $z$              | – number of electrons  |

**Greek letters**

|          |   |
|----------|---|
| $\gamma$ | – inhibitor concentration, $\text{g L}^{-1}$    |
| $\nu$    | – sweep rate, $\text{V s}^{-1}$                 |
| $\omega$ | – angular speed, $\text{rad s}^{-1}$            |
| $\sigma$ | – roughness factor of the surface, $\sigma = 2$ |
| $\theta$ | – surface coverage                              |
| $\eta$   | – inhibition efficiency, %                      |

**Subscripts**

|          |                                     |
|----------|-------------------------------------|
| $a$      | – anodic                            |
| $c$      | – cathodic                          |
| $m$      | – molar                             |
| corr     | – corrosion                         |
| A,0      | – anodic, absence of HI extract     |
| A,HI     | – anodic, presence of HI extract    |
| corr,0   | – corrosion, absence of HI extract  |
| corr,HI  | – corrosion, presence of HI extract |
| OCP      | – open circuit potential            |
| tot      | – total                             |
| $\Omega$ | – Ohmic                             |

**References**

1. Badawy, W. A., Ismail, K. M., Fathi, A. M., Corrosion control of Cu–Ni alloys in neutral chloride solutions by amino acids, *Electrochim. Acta* **51** (2006) 4182. doi: <https://doi.org/10.1016/j.electacta.2005.11.037>
2. Yoon, T., Shin, W. C., Kim, T. Y., Mun, J. H., Kim, T. S., Cho, B. J., Direct measurement of adhesion energy of monolayer graphene as-grown on copper and its application to renewable transfer process, *Nano Lett.* **12** (2012) 1448. doi: <https://doi.org/10.1021/nl204123h>
3. Bracey, C. L., Ellis, P. R., Hutchings, G. J., Application of copper–gold alloys in catalysis: Current status and future perspectives, *Chem. Soc. Rev.* **38** (2009) 2231. doi: <https://doi.org/10.1039/B817729P>
4. Milošev, I., Kosec, T., Electrochemical and spectroscopic study of benzotriazole films formed on copper, copper-zinc alloys and zinc in chloride solution, *Chem. Biochem. Eng. Q.* **23** (2009) 53.
5. Morselli, L., Bernardi, E., Chiavari, C., Brunoro, G., Corrosion of 85-5-5-5 bronze in natural and synthetic acid rain, *Appl. Phys. A* **79** (2004) 363. doi: <https://doi.org/10.1007/s00339-004-2536-y>
6. Pilić, Z., Martinović, I., Electrochemical behaviour of iron and AISI 304 stainless steel in simulated acid rain solution, *Int. J. Mater. Res.* **107** (2016) 925. doi: <https://doi.org/10.3139/146.111421>
7. Magaino, S., Corrosion rate of copper rotating-disk-electrode in simulated acid rain, *Electrochim. Acta* **42** (1997) 377. doi: [https://doi.org/10.1016/S0013-4686\(96\)00225-3](https://doi.org/10.1016/S0013-4686(96)00225-3)
8. Magaino, S., Soga, M., Sobue, K., Kawaguchi, A., Ishida, N., Imai, H., Zinc corrosion in simulated acid rain, *Electrochim. Acta* **44** (1999) 4307. doi: [https://doi.org/10.1016/S0013-4686\(99\)00146-2](https://doi.org/10.1016/S0013-4686(99)00146-2)
9. Bernardi, E., Chiavari, C., Lenza, B., Martini, C., Morselli, L., Ospitali, F., Robbiola, L., The atmospheric corrosion of quaternary bronzes: The leaching action of acid rain, *Corros. Sci.* **51** (2009) 159. doi: <https://doi.org/10.1016/j.corsci.2008.10.008>
10. Patel, K. K., Vashi, R. T., *Azadirachta indica* extract as corrosion inhibitor for copper in nitric acid medium, *Res. J. Chem. Sci.* **5** (2015) 59.
11. Grudić, V., Bošković, I., Gezović, A., Inhibition of copper corrosion in NaCl solution by propolis extract, *Chem. Biochem. Eng. Q.* **32** (2018) 299. doi: <https://doi.org/10.15255/CABEQ.2018.1357>
12. Otmačić Čurković, H., Stupnišek-Lisac, E., Takenouti, H., The influence of pH value on the efficiency of imidazole based corrosion inhibitors of copper, *Corros. Sci.* **52** (2010) 398. doi: <https://doi.org/10.1016/j.corsci.2009.09.026>
13. Feng, Y., Siow, K.-S., Teo, W.-K., Tan, K.-L., Hsieh, A.-K., Corrosion mechanisms and products of copper in aqueous solutions at various pH values, *Corrosion* **53** (1997) 389. doi: <https://doi.org/10.5006/1.3280482>
14. Milošev, I., Kosec, T., Bele, M., The formation of hydrophobic and corrosion resistant surfaces on copper and bronze by treatment in myristic acid, *J. Appl. Electrochem.* **40** (2010) 1317. doi: <https://doi.org/10.1007/s10800-010-0078-x>
15. Stupnišek-Lisac, E., Gazivoda, A., Madžarac, M., Evaluation of non-toxic corrosion inhibitors for copper in sulphuric acid, *Electrochim. Acta* **47** (2002) 4189. doi: [https://doi.org/10.1016/S0013-4686\(02\)00436-X](https://doi.org/10.1016/S0013-4686(02)00436-X)



16. Blajiev, O., Hubin, A., Inhibition of copper corrosion in chloride solution by amino-mercapto-thiazol and methyl-mercapto-thiazol: An impedance spectroscopy and a quantum-chemical investigation, *Electrochim. Acta* **49** (2004) 2761.  
doi: <https://doi.org/10.1016/j.electacta.2004.01.037>
17. Otmačić Čurković, H., Marušić, K., Stupnišek-Lisac, E., Telegdi, J., Electrochemical and AFM study of corrosion inhibition with respect to application method, *Chem. Biochem. Eng. Q.* **23** (2009) 61.
18. Allam, N. K., Nazeer, A. A., Ashour, E. A., A review of the effects of benzotriazole on the corrosion of copper and copper alloys in clean and polluted environments, *J. Appl. Electrochem.* **39** (2009) 961.  
doi: <https://doi.org/10.1007/s10800-009-9779-4>
19. de Souza, F. S., Giacomelli, C., Gonçalves, R. S., Spinelli, A., Adsorption behavior of caffeine as a green corrosion inhibitor for copper, *Mater. Sci. Eng. C* **32** (2012) 2436.  
doi: <https://doi.org/10.1016/j.msec.2012.07.019>
20. Pilić, Z., Martinović, I., Zlatić, G., Electrochemical behaviour of iron in simulated acid rain in presence of *Achillea millefolium* L., *Int. J. Electrochem. Sci.* **13** (2018) 5151.  
doi: <https://doi.org/10.20964/2018.06.29>
21. Mabrou, J., Akssira, M., Azzi, M., Zertoubi, M., Saib, N., Messaoudi, A., Albizane, A., Tahiri, S., Effect of vegetal tannin on anodic copper dissolution in chloride solutions, *Corros. Sci.* **46** (2004) 1833.  
doi: <https://doi.org/10.1016/j.corsci.2003.10.022>
22. Pilić, Z., Natural products as potential corrosion inhibitors, 17th International Conference Ružička days “TODAY SCIENCE – TOMORROW INDUSTRY”, Tomas, S., Ačkar, Đ. (ed). Proc., Faculty of Food Technology Osijek, Croatian Society of Chemical Engineers, Vukovar (2018) 11.
23. Cristofari, G., Znini, M., Majidi, L., Costa, J., Hammouti, B., Paolini, J., *Helichrysum italicum* subsp. *italicum* essential oil as environmentally friendly inhibitor on the corrosion of mild steel in hydrochloric acid, *Int. J. Electrochem. Sci.* **7** (2012) 9024.
24. Vrsalović, L., Gudić, S., Kliškić, M., Oguzie, E. E., Carev, L., Inhibition of copper corrosion in NaCl solution by caffeic acid, *Int. J. Electrochem. Sci.* **11** (2016) 459.
25. Mastelić, J., Politeo, O., Jerković, I., Contribution to the analysis of the essential oil of *Helichrysum italicum* (Roth) G. Don. – determination of ester bonded acids and phenols, *Molecules* **13** (2008) 795.  
doi: <https://doi.org/10.3390/molecules13040795>
26. Politeo, O., Jukić, M., Miloš, M., Chemical composition and antioxidant activity of essential oils of twelve spice plants, *Croat. Chem. Acta* **79** (2006) 545.
27. Tundis, R., Statti, G. A., Conforti, F., Bianchi, A., Agri-monti, C., Sacchetti, G., Muzzoli, M., Ballero, M., Menichini, F., Poli, F., Influence of environmental factors on composition of volatile constituents and biological activity of *Helichrysum italicum* (Roth) Don (Asteraceae), *Nat. Prod. Res.* **19** (2005) 379.  
doi: <https://doi.org/10.1080/1478641042000261969>
28. Seufert, G., Hoyer, V., Wollmer, H., Arndt, U., General methods and materials, *Environ. Pollut.* **68** (1990) 205.  
doi: [https://doi.org/10.1016/0269-7491\(90\)90028-B](https://doi.org/10.1016/0269-7491(90)90028-B)
29. Shen, S., Guo, X., Song, P., Pan, Y.-C., Wang, H., Wen, Y., Yang, H.-F., Phytic acid adsorption on the copper surface: Observation of electrochemistry and Raman spectroscopy, *Appl. Surf. Sci.* **276** (2013) 167.  
doi: <https://doi.org/10.1016/j.apsusc.2013.03.061>
30. Ahamad, I., Khan, S., Ansari, K. R., Quraishi, M. A., Primaquine: A pharmaceutically active compound as corrosion inhibitor for mild steel in hydrochloric acid solution, *J. Chem. Pharm. Res.* **3** (2011) 703.
31. Valcarce, M. B., de Sanchez, S. R., Vazquez, M., Localized attack of copper and brass in tap water: The effect of *Pseudomonas*, *Corros. Sci.* **47** (2005) 795.  
doi: <https://doi.org/10.1016/j.corsci.2004.07.013>
32. Babić, R., Metikoš-Huković, M., Lončar, M., Impedance and photoelectrochemical study of surface layers on Cu and Cu–10Ni in acetate solution containing benzotriazole, *Electrochim. Acta* **44** (1999) 2413.  
doi: [https://doi.org/10.1016/S0013-4686\(98\)00367-3](https://doi.org/10.1016/S0013-4686(98)00367-3)
33. Valcarce, M. B., Vazquez, M., Phosphate ions used as green inhibitor against copper corrosion in tap water, *Corros. Sci.* **52** (2010) 1413.  
doi: <https://doi.org/10.1016/j.corsci.2009.12.015>
34. Naseer, A., Khan, A. Y., A study of growth and breakdown of passive film on copper surface by electrochemical impedance spectroscopy, *Turk. J. Chem.* **33** (2009) 739.  
doi: <https://doi.org/10.3906/kim-0708-23>
35. Soltani, N., Tavakkoli, N., Khayat Kashani, M., Jalali, M. R., Mosavizade, A., Green approach to corrosion inhibition of 304 stainless steel in hydrochloric acid solution by the extract of *Salvia officinalis* leaves, *Corros. Sci.* **62** (2012) 122.  
doi: <https://doi.org/10.1016/j.corsci.2012.05.003>
36. Kadapparambil, S., Yadav, K., Ramachandran, M., Selvam, N. V., Electrochemical investigation of the corrosion inhibition mechanism of *Tectona grandis* leaf extract for SS304 stainless steel in hydrochloric acid, *Corros. Rev.* **35** (2017) 111.  
doi: <https://doi.org/10.1515/corrrev-2016-0074>
37. Ivanov, E. S., Inhibitors for Metal Corrosion in Acid Media, Metallurgy, Moscow, 1986.
38. Bouyanzer, A., Hammouti, B., A study of anti-corrosive effects of Artemisia oil on steel, *Pigment & Resin Technol.* **33** (2004) 287.  
doi: <https://doi.org/10.1108/03699420410560489>
39. de Souza, F. S., Spinelli, A., Caffeic acid as a green corrosion inhibitor for mild steel, *Corros. Sci.* **51** (2009) 642.  
doi: <https://doi.org/10.1016/j.corsci.2008.12.013>
40. Halambek, J., Berković, K., Vorkapić-Furač, J., The influence of *Lavandula angustifolia* L. oil on corrosion of Al-3Mg alloy, *Corros. Sci.* **52** (2010) 3978.  
doi: <https://doi.org/10.1016/j.corsci.2010.08.012>
41. Fouda, A. S., Al-Sarawy, A. A., Ahmed, Sh. F., El-Abbasy, H. M., Corrosion inhibition of aluminum 6063 using some pharmaceutical compounds, *Corros. Sci.* **51** (2009) 485.  
doi: <https://doi.org/10.1016/j.corsci.2008.10.012>
42. Murlidharan, S., Phani, K. L. N., Pitchumani S., Ravichandran, S., Iyer, S. V. K., Polyamino-benzoquinone polymers: A new class of corrosion inhibitors for mild steel, *J. Electrochem. Soc.* **142** (1995) 1478.  
doi: <https://doi.org/10.1149/1.2048599>
43. Bentiss, F., Traisnel, M., Lagrenee, M., The substituted 1,3,4-oxadiazoles: A new class of corrosion inhibitors of mild steel in acidic media, *Corros. Sci.* **42** (2000) 127.  
doi: [https://doi.org/10.1016/S0010-938X\(99\)00049-9](https://doi.org/10.1016/S0010-938X(99)00049-9)